ELSEVIER

Computers and Chemical Engineering 25 (2001) 509–515

Computers & Chemical Engineering

www.elsevier.com/locate/compchemeng

Dynamic simulation and optimisation of tubular polymerisation reactors in gPROMS

M. Asteasuain, S.M. Tonelli, A. Brandolin, J.A. Bandoni *

Planta Piloto de Ingeniería Química (PLAPIQUI)-UNS-CONICET, Camino La Carrindanga km 7, 8000 Bahía Blanca, Argentina

Received 10 May 2000; accepted 5 January 2001

Abstract

In this paper a dynamic model of the high-pressure polymerisation of ethylene in tubular reactors is introduced and a dynamic optimisation problem is formulated for studying start-up strategies. The optimisation objectives proposed are to maximise outlet conversion and optimise the time necessary for it's stabilisation while keeping product molecular properties between commercial ranges. Results are shown giving the time responses for temperature, number-average molecular weight and conversion along the reactor axial distance, which were obtained using different control variable profiles. Improving in reactor productivity is achieved. The interface gOPT of the gPROMS simulator was used to resolve the optimisation problem and to perform the simulations.

Keywords: Polymerisation reactors; Polyethylene; Mathematical modelling; Reactor optimisation; gPROMS; Dynamic simulation

1. Introduction

High-pressure polymerisation of ethylene to produce low-density polyethylene in tubular reactors is a widely used industrial process. It is carried out under rigorous operating conditions, and consequently a mathematical model is an attractive tool to study safely and economically the influence of the different design and operative variables on production performance and product quality. Several authors have presented different models dealing with the stationary state of this process (Zabisky, Chan, Gloor & Hamielec, 1992; Brandolin, Lacunza, Ugrin & Capiati, 1996). However, less attention has been paid to the dynamic behaviour of this reactor, despite a dynamic model may be successfully used to study start-up and shutdown strategies and production optimisation.

This type of tubular reactor has a main feed consisting in ethylene monomer, solvent, inerts and oxygen initiator. In addition, there are lateral injections of initiators consisting in peroxide with or without monomer. The reactor is divided in heating/cooling jacket zones in order to reach an appropriate reaction temperature or to control the exothermic reaction. Even though there is a general tendency to avoid pulsing the reactor, this mode of operation is still in use in some industrial reactors. In those cases, a pulse valve is located at the exit to control polymer build-up at reactor walls. This last feature accounts for an inherent oscillating temperature profile due to uncertain values of heat transfer coefficients. Other common disturbances in this process occur due to changes in temperature levels in the jacket fluid and concentration of impurities in the monomer feed. In industry, normally a single reactor is used to produce several kinds of polyethylenes of different molecular characteristics, making them appropriate for different final uses. Consequently, such type of reactor must be flexible enough to deal with a wide range of operating conditions.

In industrial reactors whole temperature profiles and in particular peak temperatures values are controlled by manipulation of feed temperature and pressure, telogen and initiator flow rates as well as their compositions. Keeping the peak temperatures within a certain range ensures the production of a desired polymer grade. The telogen, which acts as a chain transfer agent, is used specially to control the molecular weight of the polymer being produced.

* Corresponding author. Tel.: +54-91-4861700; fax: +54-91-4861600.

E-mail address: abandoni@plapiqui.edu.ar (J.A. Bandoni).

0098-1354/01/$ - see front matter
PII: S0098-1354(01)00631-7

The main objective of our study is to analyse the start-up and shutdown strategies and perform flexibility analysis in the polymerisation reactor. The considered control variables were the initiator and telogen flow rates. For this paper, we developed a dynamic model that predict average molecular weights, monomer conversion, concentrations and temperature as function of time and axial reactor length. The simulation package gPROMS (Barton & Pantelides, 1994) was used to perform these studies. Then, the interface gOPT of gPROMS was used to resolve the start-up optimisation problem.

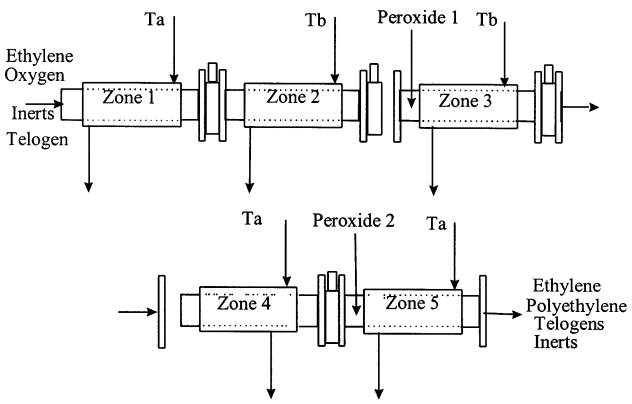

Fig. 1. Tubular reactor for high-pressure ethylene polymerisation.

Table 1
Design features and steady state operating conditions for the base case

Length/diameter (L/D)	27 800
Internal diameter (D)	0.05 m
Number of zones (Nz)	5
Zone axial length/diameter (Lz_i/D, $i = 1..5$)	1200, 2000, 3600, 10 200, 10 800
Inlet temperature	76°C
Inlet pressure	2250 atm
Jacket temperatures $T_{j,1} = T_{j,4} = T_{j,5} = \text{Ta}$	168°C
Jacket temperatures $T_{j,2} = T_{j,3} = \text{Tb}$	225°C
Specific heat of reacting mixture (Cp_i $i = 1$,..., Nz)	0.58, 0.58, 0.75, 0.75, 0.96 cal/g °C
Global heat transfer coefficient (U_i $i = 1$,..., Nz)	2.6×10^{-2}, 2.6×10^{-2}, 2.0×10^{-2}, 1.5×10^{-2}, 4.7×10^{-3} cal/cm^2 °C s
Density of reacting mixture (ρ)	0.53 g cm^3
Monomer flow rate	11 kg s^{-1}
Oxygen flow rate	6.8×10^{-5} kg/s
Telogen flow rate	7.4×10^{-2} kg/s
Inert flow rate	2.2×10^{-1} kg/s
Initiator 1 flow rate	1.0×10^{-3} kg/s
Initiator 2 flow rate	1.6×10^{-4} kg/s
Conversion	30%
Mn	21 900 g/mol

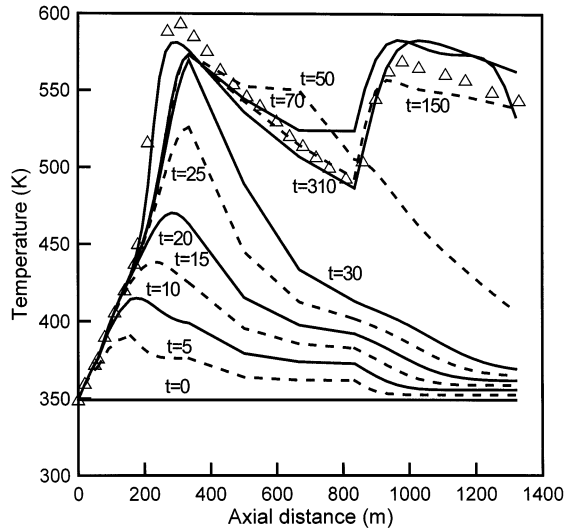

Fig. 2. Axial temperature profiles. Calculated during start-up for Policy A (lines). Parameter, time in seconds. Measured steady-state temperature profile for the base case (△).

2. Model description

2.1. Reactor model

The considered reactor configuration is displayed in Fig. 1. It corresponds to a typical industrial reactor with a length to diameter ratio of around 20 000. The unit operates at very severe conditions, high axial velocities (around 11 m/s), temperatures ranging from 50°C at the reactor entrance to 325°C at the peaks, and pressures between 1800 and 2800 atm. Temperature along the reactor is usually recorded by means of several thermocouples located along the axial distance. The specific design and operating conditions employed in this work are reported in Table 1. In this case more than 100 thermocouples were employed to record the temperature profile, which is shown in Fig. 2 (triangles).

For simulation purposes, the reactor model was divided in five zones. A different zone starts when there is a change in the level of jacket temperature or when an initiator injection occurs. The physical properties considered are density and specific heat. They are regarded as constant in each zone, and their values have been obtained by averaging simulation results of the rigorous, steady state model (Brandolin, Lacunza, Ugrin & Capiati, 1996). The velocity of the reaction mixture and global heat transfer coefficient were also considered constant at each zone and their values obtained by the same procedure. The fluid in the jacket (vapour in the first zone and liquid water in the others) enters counter flow with respect to reaction mixture. For simplicity we considered that jacket temperature remains constant at each zone and equal to the average between the inlet and output jacket temperature of the corresponding

zone (see Table 1). For the steady state condition, Asteasuain, Pereda, Lacunza, Ugrin and Brandolin (2001) have already shown that considering the jacket temperature constant by zones allows a good prediction of temperature profiles for the reacting mixture. Ethylene monomer (M), which contains inerts, oxygen and telogen (S), enters at the beginning of the reactor. The first two jacket zones are used to heat the mixture up to the optimal temperature for the first peroxide feeding. Meanwhile oxygen begins to produce initiator radicals, which propagate to form long macromolecules. After peroxide enters the third zone the reaction explode reaching a temperature peak, then the fourth zone is used to cool down the mixture to the optimal level for the second initiator injection in the fifth zone where the reaction proceeds again. Adding telogen at the reactor entrance avoid the production of prohibitively large polymer molecules which would increase viscosity interfering with heat transfer and with the thermal control of the reactor. The initiator flow rates are the one that determines the level of reactor conversion, but there is a limit to the quantity to be added because reactor runaway is always possible.

2.2. Kinetic mechanism

Table 2 shows the basic reactions considered in our model. Oxygen and organic peroxide (I) decomposition (Eqs. (1) and (2)) generate initiation radicals when reactor temperature reaches appropriate levels. Propagation reaction takes place when monomer (M) reacts with radicals to produce a growing macromolecule (Eq. (3)). This reaction accounts for most of the polymerisation heat, which is 21 500 cal/mol. Natural termination is produced by combination of two radicals (Eq. (4)) or by thermal degradation (Eq. (5)). A chain transfer agent (telogen) is commonly fed at the reactor inlet in order to control molecular weight. Telogens (S) react with radicals producing a dead polymer and an initiation radical (Eq. (6)). In consequence, the presence of telogen results in shorter macromolecules. Another reactions, such as transfer to polymer and intermolecular scissions are also important in this polymerisation. They affect long and short-chain branching, and weight-average molecular weights. Up to this point, we are only concerned with conversion and number-average molecular weight predictions, so the last reactions were not included in the model

Table 2
Basic kinetic mechanism

Oxygen initiation		Peroxide (I) initiation	
$O_2 + M \xrightarrow{k_o} 2R_1(0)$	(1)	$I \xrightarrow{fk_d} 2R_1(0)$	(2)
Propagation		Termination by combination	
$R_i(x) + M \xrightarrow{k_p} R_i(x+1)$	(3)	$R_i(x) + R_j(y) \xrightarrow{k_{tc}} P_{i+j-1}(x+y)$	(4)
Thermal degradation		Chain transfer to telogen (S)	
$R_i(x+1) \xrightarrow{k_{tdt}} P_i(x) + R_1(0)$	(5)	$R_i(x) + S \xrightarrow{k_{trs}} P_i(x) + R_1(0)$	(6)

In Table 2, M is the ethylene monomer, $R_i(x)$ and $P_i(x)$ represent radical and dead polymer of chain length x and i long-chain branching, respectively. Kinetic constants (k) follow the Arrhenius law in temperature. The corresponding values were taken from Brandolin, Lacunza, Ugrin and Capiati, (1996) and Asteasuain, Pereda, Lacunza, Ugrin and Brandolin (2001).

2.3. Mass and energy balances

Eq. (7) presents the mass balance of a generic component 'j', and Eq. (8) the energy balance. The corresponding initial and boundary conditions are given in Eqs. (9) and (10).

Component concentration (C_j):

$$\frac{\partial C_j}{\partial t} = r_j - v\frac{\partial C_j}{\partial x} \quad j = 1, N_{\text{comp}}$$

$$C_j\text{: } [O_2], [M], [Ra], [\text{Pol}], [S], [I], [\text{Inerts}] \tag{7}$$

where $[Ra]$ and [Pol] stand for global concentrations of radicals and polymer, respectively.

Reactor Temperature (T):

$$\rho C_p \frac{\partial T}{\partial t} = -\rho C_p v\frac{\partial T}{\partial z} - \frac{4U(T-T_j)}{D_i} + k_p[Ra][M](-\Delta H) \tag{8}$$

where ρ, reacting mixture density; C_p, specific heat; v, axial velocity; U, global heat transfer coefficient; T_j, jacket temperature; D_i, inside diameter.

Initial conditions

$$t = 0 \quad \begin{cases} C_j(0, z) = C_{j0}(z) \\ T(0, z) = T_0(z) \end{cases} \tag{9}$$

Boundary conditions

$$z = 0 \quad \begin{cases} C_j(t, 0) = C_{j\text{in}}(t) \\ T(t, 0) = T_{\text{in}}(t) \end{cases} \tag{10}$$

Monomer conversion and number-average molecular weight are calculated from simulation results, by means of Eqs. (11) and (12), respectively.

Monomer conversion

$$X(t, L) = 1 - \sum_{j=1,\, j\neq \text{pol}}^{N_{\text{comp}}} [C_j]_{wt/wt}(t, L) \tag{11}$$

Number-average molecular weight

$$\mathrm{Mn}(t, L) = \frac{X(t, L)\rho(L)}{[\mathrm{Pol}](t, L)} \tag{12}$$

2.4. Dynamic optimisation problem

As it was mentioned earlier, the main objective of this work is to find optimal start-up and shutdown policies for the reactor. From the operating point of view this means reaching the maximum product conversion and the steady state operation in a minimum time. Mathematically this situation can be represented by a dynamic optimisation problem.

In a start-up policy the objective function to be maximised is the monomer conversion at the reactor exit, $X(t_f, L)$ (where X is the monomer conversion, t_f the final time and L the reactor length). The mathematical statement of this model is as follows (Eqs. (13)–(21)).

Objective function

$$\underset{t_f, \bar{u}(t,z)}{\mathrm{Max}} X(t_f, L) \tag{13}$$

subject to:

Process model:

$$F(\bar{v}(t,z), \dot{\bar{v}}_z(t,z), \dot{\bar{v}}_t(t,z), \bar{u}(t,z), \bar{w}(t,z)) = 0 \tag{14}$$

Initial conditions:

$$I(\bar{v}(0,z), \dot{\bar{v}}_z(0,z), \dot{\bar{v}}_t(0,z), \bar{u}(0,z), \bar{w}(t,z)) = 0 \tag{15}$$

Boundary conditions:

$$B(\bar{v}(t,0), \dot{\bar{v}}_z(t,0), \dot{\bar{v}}_t(t,0), \bar{u}(t,0), \bar{w}(t,z)) = 0 \tag{16}$$

Time horizon bounds:

$$t_{f,\min} \le t_f \le t_{f,\max} \tag{17}$$

Control variable ($\bar{u}$) bounds:

$$\bar{u}_{\min} \le \bar{u}(t, z) \le \bar{u}_{\max} \tag{18}$$

Dependent variables bounds

$$\bar{v}_{\min} \le \bar{v}(t,z) \le \bar{v}_{\max}, \qquad \bar{w}_{\min} \le \bar{w}(t, z) \le \bar{w}_{\max} \tag{19}$$

$$z \in [0, L] \tag{20}$$

$$t \in [0, t_f] \tag{21}$$

where $\bar{u}(t, z)$, vector of control variables; $\bar{w}(t, z)$, vector of algebraic state variables; $\bar{v}(t, z)$, vector of differential state variables; t, time; z, axial length. In what follows $\bar{w}(t, z)$ and $\bar{v}(t, z)$ are combined in a single vector $\bar{x}(t, z)$.

2.5. Solution of the optimisation problem

The model is represented by a system of partial differential algebraic equations (PDAE), with path constraints and bounds on independent variables. It was solved using the general purpose modelling, simulation and optimisation package gPROMS (generalised PROcess Modelling System). In gPROMS, the model of each unit operation contains all the information regarding to the physicochemical behaviour of the system and the design characteristics of the equipment. On the other hand, external actions affecting the unit are declared independently. This allows the use of the same model of equipment each time it is repeated within the same process. Taking advantage of this property, the reactor was simulated as a series of tubular reactors. Each one represents a section, which is determined by a different level in jacket temperature or a lateral feed.

The dynamic optimisation strategy within gPROMS is the DAEOPT code that implements the algorithm outlined by Vassiliadis, Sargent and Pantelides (1994a,b). The package automatically discretized the spatial variable, axial distance, according to the options provided by the user. In our case, the problem was solved using backward finite differences. The resulting DAE system was then solved using the DASOLV code while the optimisation is carried out by the SRQPD code. The interface called gOPT makes it possible to perform dynamic optimisation calculations using DAEOPT and processes defined in the gPROMS language.

To check the reactor model validity, several simulation runs were performed for different initial conditions. It was observed, in all cases, that the temperature and component's concentrations, as well as monomer conversion and number-average molecular weight evolved towards the expected values of steady state obtained with an existing rigorous reactor model (Brandolin, Lacunza, Ugrin & Capiati, 1996).

3. Results and discussion

As we already mentioned, Table 1 shows the main design features and the steady-state base case operating conditions of the industrial reactor under analysis. These conditions lead to a product of commercial value. The corresponding measured steady-state monomer conversion and number-average molecular weight are also shown. In order to obtain this steady state, we consider that at time zero the reactor contains only monomer, oxygen and telogen at a temperature and concentrations equal to those of the main feed. We also assume that the input flow rates are fixed at their final steady-state values in the base case.

To optimise the reactor operation, we analyse different start-up policies that maximise conversion keeping the molecular weight close to the value of the base case. As it was stated before, initiator and telogens flow rates were used as control variables. Initiator flow rates mainly determine conversion level and temperature profiles while telogen flow rate controls number average molecular weight. Tables 3 and 4 show the particular

Table 3
Optimisation conditions for Policy A

Policy A	Piecewise constant control vector $\bar{u}$, over four different and adjustable time intervals within [0, t_f]
Minimum start-up period ($t_{f,min}$)	100 s
Maximum start-up period ($t_{f,max}$)	350 s
Control vector ($\bar{u}$)	[$F_{I,1}$, $F_{i,2}$, F_s] (kg/s)
$\bar{u}$ lower bound ($\bar{u}_{min}$)	[5×10^{-5}, 5×10^{-5}, 5×10^{-5}] (kg/s)
$\bar{u}$ upper bound ($\bar{u}_{max}$)	[5×10^{-3}, 2×10^{-3}, 5×10^{-1}] (kg/s)
Differential and algebraic variables s.t. bounds ($\bar{x}$)	[$T(t, z)$, Mn(t_f, L)]
$\bar{x}$ lower bound ($\bar{x}_{min}$)	[N/A, 21 900 g/mol]
$\bar{x}$ upper bound ($\bar{x}_{max}$)	[330°C, 24 000 g/mol]

Table 4
Optimisation conditions for Policy B

Policy B	Piecewise linear $\bar{u}$, over five different and adjustable time intervals within [0, t_f]
Minimum start-up period ($t_{f,min}$)	100 s
Maximum start-up period ($t_{f,max}$)	350 s
Control vector ($\bar{u}$)	[$F_{I,1}$, $F_{i,2}$, F_s] (kg/s)
$\bar{u}$ lower bound ($\bar{u}_{min}$)	[5×10^{-5}, 5×10^{-5}, 5×10^{-5}] (kg/s)
$\bar{u}$ upper bound ($\bar{u}_{max}$)	[5×10^{-3}, 2×10^{-3}, 5×10^{-1}] (kg/s)
Differential and algebraic variables s.t. bounds ($\bar{x}$)	[$T(t, z)$, Mn(t, L)]
$\bar{x}$ lower bound ($\bar{x}_{min}$)	[N/A, 21 900 g/mol]
$\bar{x}$ upper bound ($\bar{x}_{max}$)	[330°C, 24 000 g/mol]

variables and values employed in Eqs. (13)–(21) for two different optimisation policies. Values not consigned in those tables remain equal to the ones of Table 1. The main difference between these two policies is the way in which the molecular weight is checked. In policy A, the molecular weight is checked only at the final start-up time, but in policy B it is done at the end of each time interval. In this way one should expect to obtain a suitable value of molecular weight over a wider time period.

Figs. 2–9 show results corresponding to the optimal start-up policies A and B detailed in Tables 3 and 4, respectively.

As it was already mentioned, the reactor was divided in five zones. The first zone is used to preheat the reaction mixture up to the temperature where oxygen initiates the reaction. In the second zone, propagation occurs due to radicals generated by oxygen.

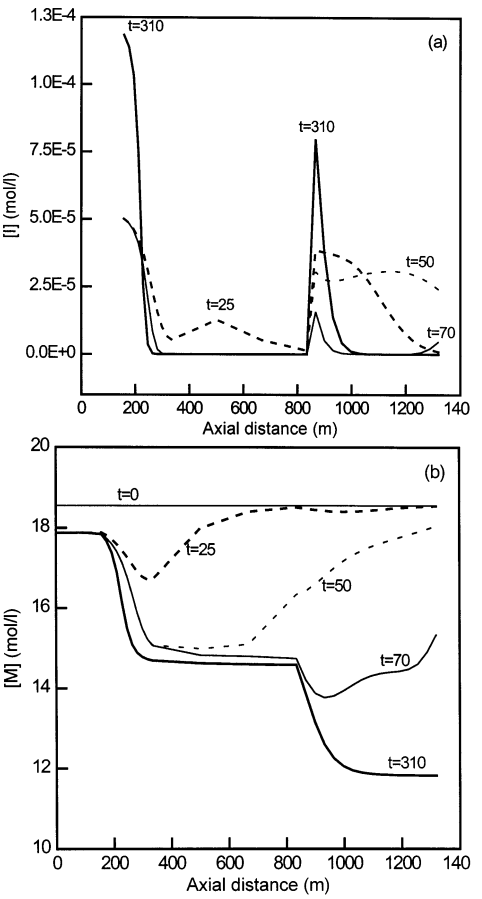

Fig. 3. (a) Axial profiles of initiator concentration. (b) Axial profiles of monomer concentration. Both calculated during start-up for Policy A. Parameter, time in seconds.

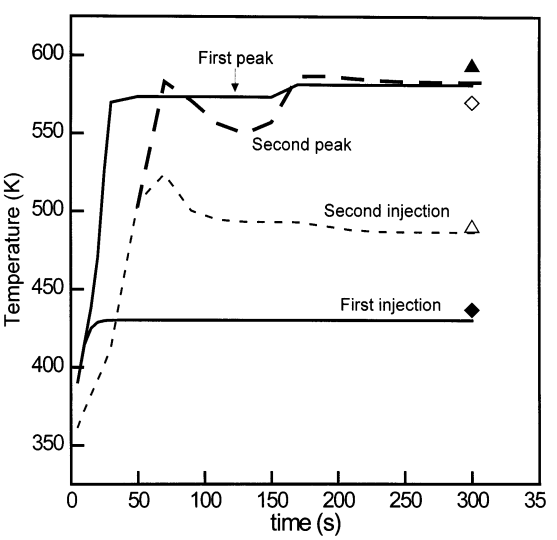

Fig. 4. Calculated time evolution of peak and injection temperatures during start-up for Policy A (lines). Measured first (▲) and second (◇) peak temperature, and first (◆) and (△) second injection temperature for the steady-state base case.

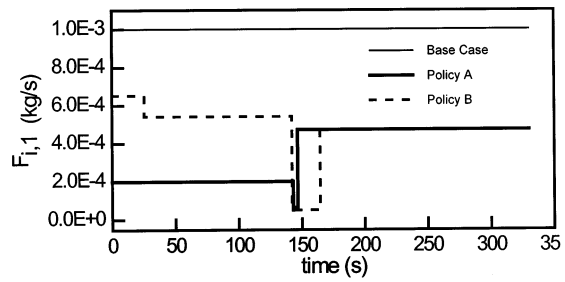

Fig. 5. Calculated first peroxide feed flow rate vs. start-up time.

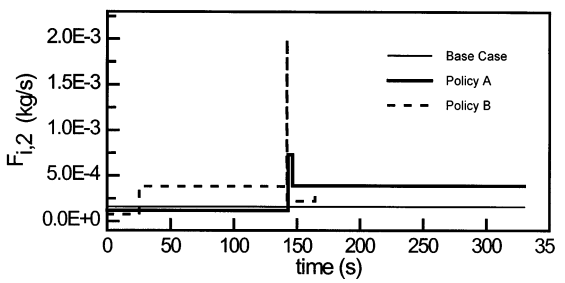

Fig. 6. Calculated second peroxide feed flow rate vs. start-up time.

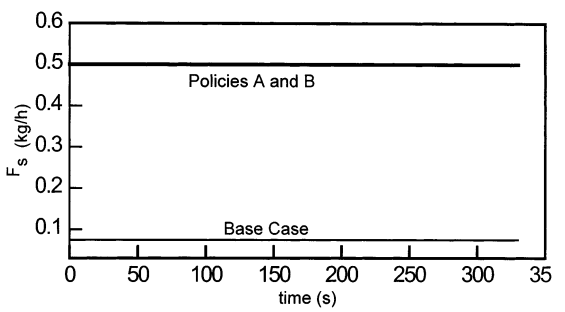

Fig. 7. Calculated telogen flow rate vs. start-up time.

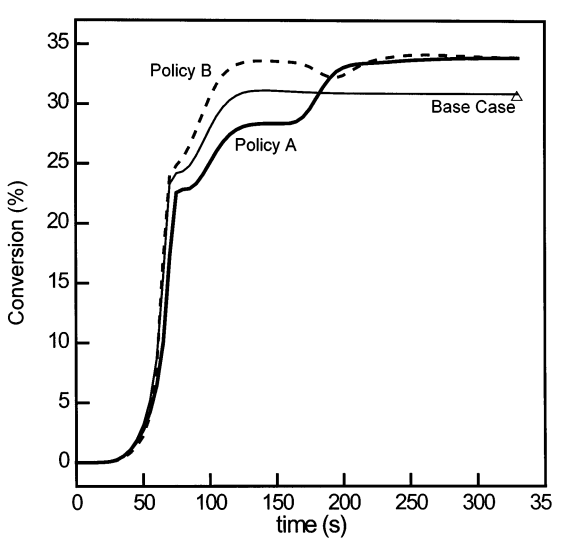

Fig. 8. Calculated conversion at reactor exit vs. start-up time (lines). Steady-state measured conversion for base case (△).

Two different peroxide initiators are injected at the beginning of the third and fifth sections generating two reaction zones, respectively. The fourth zone is used for cooling the reacting mixture. Most of the polymerisation occurs in the third and fifth zones due to the short lifetime of the initiators. For policy A, axial temperature profiles as well as profiles of initiator and monomer concentrations, are presented using time as parameter, in Figs. 2 and 3a and b, respectively. Temperature evolves rapidly from a constant profile to the one typical of these reactors (one peak for every initiator injection). For comparison purposes, Fig. 2 also shows the steady-state measured temperature profile for the base case, which is close to the final calculated constant profile for Policy A. It is necessary to reach a certain temperature level at the end of the heating section or cooling zones in order the initiator to be able to generate enough radicals to initiate the reaction. When this occurs, the sharp increase in temperature is in accordance with initiator and monomer profiles. As expected, an explosive generation of radicals appears after the initiator injection. The variations of temperature profiles are also related to changes in initiator flow rates. Temperature peaks become higher and steeper when initiator flow rate increases. An increase on final conversion is expected in this case. On the other hand, a downstream displacement of the reaction zone with less monomer consumption is expected when initiator flow rate decreases. On the other hand, Fig. 4 shows the evolution in time of the temperatures at the peak and injection points. As expected, at the first reaction section these temperatures accommodate faster and more smoothly than the ones corresponding to the second reaction section. All the values compare well with the corresponding measured temperatures reported for the base case. Figs. 5–7 present the optimal initiator and solvent fluxes for the base case and for both optimal policies. Fluxes at the last interval were the same for both policies, since they correspond to the best combination that leads to a maximum steady-state conversion. When molecular weight is only controlled at the final start-up time (Policy A), initiator fluxes (Figs. 5 and 6) start at a low value in the first interval and the highest values appear in the last interval. If molecular weight is controlled through the start-up (Policy B), specifically in each interval extreme, it is necessary to start with a higher initiator flow rate which value is similar to the one for the final interval. In both cases the optimum telogen flow rate was at its maximum allowed level.

It is known that when polymerisation starts, very high molecular weight polymer is produced. This is the situation at the beginning of the start up, as it is shown in Fig. 8. In other aspects, when telogen flux is high enough, it is possible to obtain low molecular weight in the range of the corresponding commercial values.

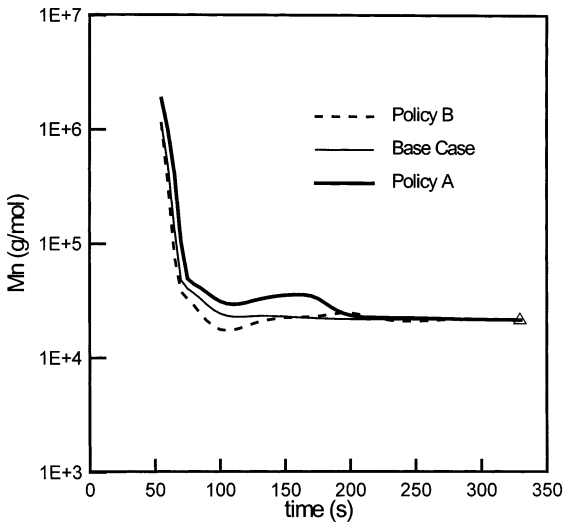

Fig. 9. Calculated number-average molecular weight of the product (Mn) vs. start-up time (lines). Steady-state measured Mn for base case (△).

Figs. 8 and 9 present the evolution of conversion and number-average molecular weights at the reactor outlet during the start-up. Both start-up policies determine an increase of around 3% in conversion level with respect to the base case. Conversion reaches its highest value more rapidly in Policy B. As mentioned before, at the beginning of the reaction the product molecular weight increases rapidly to an extremely high value. This behaviour makes very difficult to maintain the molecular weight within the desired range when the optimisation routine tries to force Mn to lie between the limits set at the end of each time interval. This result in an oscillatory behaviour, which presents values that are appropriate at the checkpoints, but are far from the limits between them. Nevertheless, the latter policy produces polymer at the desired molecular weight value over a wider portion of the start-up time than policy A.

4. Conclusions

The optimal start-up policies found in this work lead to maximum conversion values that are above the commonly conversions levels for this type of reactors. Reactor safe operation was guaranteed by means of a restriction in maximum operating temperature and the maximum conversion is moderate enough to ensure good heat transfer avoiding undesirable increments in reactor viscosity. Moreover, reactor productivity was increased while maintaining commercial valuable product molecular weight. Work is under way to determine shutdown strategies following procedures similar to the ones outlined in this work.

Acknowledgements

The authors gratefully acknowledge the financial support given by CONICET (the Argentinian National Research Council) and UNS (National University of the South).

References

Asteasuain, M., Pereda S., Lacunza, M. H., Ugrin P. E., & Brandolin, A. (2001). Industrial high-pressure ethylene polymerisation initiated by peroxide mixtures. A reduced mathematical model for parameter adjustment. *Polymer Engineering and Science*, in press.

Barton, P. I., & Pantelides, C. C. (1994). Modeling of combined discrete/continuous processes. *American Institute of Chemical Engineering Journal*, *40*(6), 966–979.

Brandolin, A., Lacunza, M. H., Ugrin, P. E., & Capiati, N. J. (1996). High-pressure polymerisation of ethylene. An improved mathematical model for industrial tubular reactors. *Polymer Reaction Engineering*, *4*(4), 193–241.

Vassiliadis, V. S., Sargent, R. W. H., & Pantelides, C. C. (1994a). Solutions of a class of multistage dynamic optimisation problems. 1. Problems without path constrains. *Industrial Engineering and Chemical Research*, *33*(9), 2111–2122.

Vassiliadis, V. S., Sargent, R. W. H., & Pantelides, C. C. (1994b). Solutions of a class of multistage dynamic optimisation problems. 2. Problems with path constrains. *Industrial Engineering and Chemical Research*, *33*(9), 2123–2133.

Zabisky, R. C. M., Chan, W.-M., Gloor, P. E., & Hamielec, A. E. (1992). A kinetic model for olefin polymerisation in high-pressure tubular reactors: a review and update. *Polymer*, *33*(11), 2243–2262.